Research on Chemical Intermediates (2019) 45:4053–4066
https://doi.org/10.1007/s11164-019-03890-5

Photo- and temperature-dependent formation of tryptophan/silver nanoparticles

Iu. Mukha[1] · N. Vityuk[1] · A. Khodko[2] · O. N. Kachalova[2,4] · O. Fedyshyn[3] · M. Malysheva[3] · A. Eremenko[1]

Received: 3 February 2019 / Accepted: 13 April 2019 / Published online: 19 June 2019

Abstract

Amino acid tryptophan is an advantageous reagent for preparation of biocompatible noble metal nanoparticles as promising anticancer agents. The reduction of metal ions in the presence of tryptophan proceeds through the indole moiety of the molecule. The formation of silver nanoparticles, namely the redox process between Ag^+ and Trp, was activated by UV-C LED irradiation at 278 nm, corresponding to the position of the indole absorption band. The experimental parameters of irradiation were varied systematically aiming to influence the kinetics of the process and properties of prepared Ag nanoparticles. The dependence of optical spectra and size distribution of Ag nanoparticles on temperature of reaction (25, 40 and 60 °C) and output optical power density (0.4, 0.6 and 1.0 mW/cm^2) were investigated by UV–vis absorption spectroscopy and dynamic light scattering data. Under UV irradiation, the rate of Ag nanoparticles formation can be accelerated by a factor of 10 with increase of the temperature from 25 to 60 °C, leading to the shift of plasmon absorption band maxima from 422 to 412 nm. The optimal UV irradiation parameters and temperature of reaction can be a basis for preparing colloids with tailored dispersity and optical properties.

Keywords Biocompatible silver nanoparticles · Tryptophan · Photochemical synthesis

Introduction

Noble metal nanoparticles (NPs), namely gold and silver, continue to attract attention as promising agents used for delivery, sensing and treatment of tumors [1, 2]. Over the past decade, the various metal-based functional nano-objects and smart nanomaterials were synthesized and extensively studied in the Laboratory of Photonics of Oxide Nanosystems (Chuiko Institute of Surface Chemistry of NAS of

✉ Iu. Mukha
iu.mukha@gmail.com

Extended author information available on the last page of the article

Ukraine) Among them, the stable colloids of silver, gold and their bimetallic composites obtained in the presence of amino acid tryptophan (Trp), were shown as effective biocompatible nanosystems with a huge perspective for further applications in cancer treatment without the need of further functionalization with specific moieties for targeted delivery [3–6]. Different toxic and anti-cancer effects of noble metal nanoparticles were fixed depending on their composition.

Proposed experimental procedure allows preparing noble metal colloids with prolonged stability where nanoparticles maintain optical properties and nanodimension. The chemical process conducted at the temperature of boiling solution promotes quite broad size distribution according to a dynamic light scattering (DLS) method by intensity basis that was caused by diffusion interaction of formed particles. It is known that size of nanoparticles is one of the key factors that effects greatly their biological activity due to the different mechanisms involved during the interaction with the cell. Thus, changing the size of NPs we can improve the anti-cancer effect. We believe that properties of NPs in the studied system can be controlled with lower temperatures by applying UV irradiation. Here, we consider monometallic silver nanoparticles (Ag NPs) in a series of silver/gold mono- and bimetallic nanosized systems.

The chemical synthesis of stable Ag/Trp NPs requires boiling temperature for the activation of redox reaction between metal ions and amino acid. Since the process involves the photoactive indole ring of Trp, the additional photoactivation of the system with UV irradiation can induce the process and speed up the particle formation under lower temperatures.

The deep ultraviolet light emission diodes (UV-C LED) were used as an advantageous source for the photoinduced synthesis of Ag colloids in an Ag/Trp system, since the system can be activated with precise wavelength, namely at 278 nm, exactly corresponding to the absorbance maximum of indole moiety of Trp. Therefore, we can affect the rate of reaction with further control of Ag NPs characteristics using different parameters of UV irradiation of the reaction mixture that play a determining role for the effectiveness of sensing and treatment.

This paper is focused on optical properties, connected to morphology and size distribution of Ag NPs produced during photochemical reaction between Ag^+ and Trp under varied experimental conditions (optical power density, duration of UV irradiation, temperature) studied by UV–vis absorption spectroscopy, transmission electron microscopy and dynamic light scattering.

Experimental

The silver nanoparticles were formed during the chemical and photochemical processes. The typical synthesis of Ag NPs in the presence of tryptophan was conducted in a 1 cm^2 quartz cuvette ($V = 3$ ml) using silver nitrate ($AgNO_3$) and amino acid tryptophan (Trp) in an aqueous medium at the concentration of $C = 1 \times 10^{-4}$ M and molar ratio Ag:Trp = 1:1. The pH of the system pH = 10 was reached with the 1 N solution of NaOH. The initial solutions of Trp were heated to the given temperature ($T = 25$ °C, 40 °C and 60 °C) in 1 cm quartz cuvettes. Then $AgNO_3$ was

added and the system was immediately irradiated by UV-C LED. The obtained systems were compared with colloid formed during the chemical reaction between Ag^+ and Trp in alkaline medium from a boiling aqueous solution according to procedure described in [4].

For the photochemical activation, we applied UV-C LED source (LGInnotek) with the wavelength of $\lambda = 278$ nm at output optical power density of $P = 1.0 \pm 0.1$ mW/cm^2. The synthesis was conducted at 25, 40 and 60 °C using the UV-C LED parameters mentioned above. Solutions were irradiated during 2–5 h depending on the sample reaching the moment of the maximal value of the optical density of the absorption band of localized surface plasmon resonance (LSPR or plasmon band). The reaction proceeded for 2, 3 and 5 h under heating at 60 °C, 40 °C and 25 °C, respectively.

For the set of experiments, the synthesis was conducted at 60 °C under UV irradiation with optical power density of 0.4, 0.6 and 1.0 mW/cm^2 at the wavelength of $\lambda = 278$ nm.

The absorption spectra of colloids obtained by both chemical and photochemical methods were recorded in the UV–visible region by a spectrophotometer Lambda 35 (Perkin-Elmer, United States) in 1 cm quartz cells, in the equal time intervals of reaction starting from t_0—the moment when reagents were mixed.

The particle size distribution function was studied by a laser correlation spectrometer Zeta Sizer Nano S (Malvern, UK) equipped with a correlator (Multi Computing Correlator Type 7032 CE) by the dynamic light scattering (DLS). The helium–neon laser LGN–111 was used with the output power of 25 mW and wavelength of 633 nm to irradiate the suspension. The registration and statistical processing of the scattered laser light at 173° from the suspension were performed three times for 120 s at 25 °C. The resulting autocorrelation function was treated with standard computer programs PCS–Size mode v.1.61.

Results and discussion

The optical spectrum of silver nanoparticles (Ag NPs) is characterized by an absorption band of LSPR in a visible range with a maximum of about 400 nm. For the Ag/Trp system, as we showed earlier [4], it is possible to obtain stable silver colloids with plasmon band maximum at 417 nm. Such colloids are formed during the chemical reaction between Ag^+ and Trp in alkaline medium from boiling solution (Fig. 1a). The bands in the UV region, namely at 270–290 nm, correspond to the absorption of Trp and its oxidation products formed during reaction.

The oxidation of amino acid in studied systems in chemical process proceeds through indole ring cleavage, as was shown by the authors in [7]. During the photochemical process the direct activation occurs with precise wavelength that corresponds to the indole ring band. Thus, we assumed that the photochemical oxidation of Trp follows via the kynurenine pathway through indole ring cleavage as well.

The decrease of the temperature of the chemical reaction in the Ag/Trp system significantly slowed down the metal reduction process and, in turn, the particle formation. In comparison to the chemical reaction occurring at 100 °C, the silver

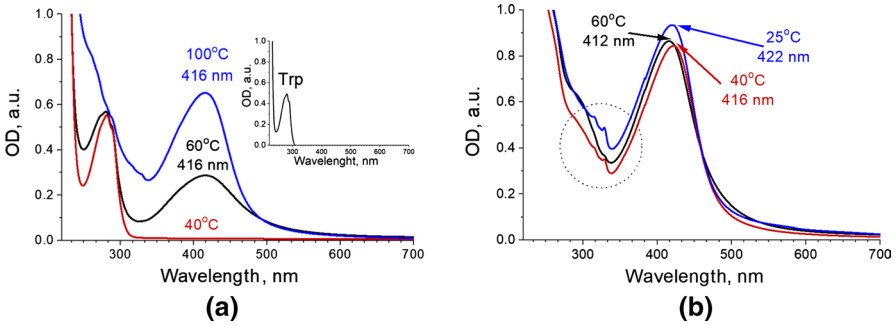

Fig. 1 The optical density of Ag NPs colloids obtained in the presence of tryptophan at different temperatures without (**a**) and with (**b**) UV-C irradiation at 278 nm with output optical power density of 1.0 mW/cm^2 after a week of storage. Inset: the absorption spectrum of Trp

plasmon band was wide and low intense after the reaction at 60 °C after 120 min while the plasmon absorption band was not observed at 25–40 °C (Fig. 1a).

When irradiation at 278 nm was applied to the Ag/Trp system, we observed an intense silver plasmon band of Ag NPs formed not only at 60 °C, but also at 40 °C and 25 °C (Fig. 1b).

In photochemical reaction the temperature influenced the particle formation process. Depending on the temperature, we observed the changes in plasmon band growth rate, optical density, the position of band maxima and other characteristics such as plasmon band width and total shape of the spectrum.

To understand the reasons for the abovementioned changes in the optical characteristics of formed silver NPs, we analyzed some time-dependent parameters illustrated in Fig. 2. The intensity increase of the silver absorption band proceeded much faster at higher temperatures (Fig. 2a). It required more than 4 h to reach the maximum optical density of the silver plasmon band at 25 °C. Twice less time, 2 h, was needed for the reaction at 40 °C, and the fastest rate of the reaction (30 min) was observed at 60 °C.

The time-dependent spectra reflecting LSPR growth were analyzed using exponential-based functions (Table 1). According to calculated time constants, the formation of NPs under UV illumination at $\lambda = 278$ nm occurred app. 2.4 times faster with the increase of the temperature from 25 to 40 °C and four times faster—from 40 °C to 60 °C. The most rapid process conducted at 60 °C was characterized with further linear decay of optical density at LSPR maximum after 50 min of reaction. The kinetics of optical density growth match the sigmoidal [8] growth profile (Adj-$R^2 = 0.9984$) which is in better agreement with experimental values compare to exponential fit (Adj-$R^2 = 0.9668$). The Adj-R^2 is an estimate of goodness of fit and this value is suitable for comparing the different fitting models.

The particles formation in solution follows through the processes of nucleation, coalescence of nuclei and growth of NPs [8]. The latter could be due to Ostwald ripening, coalescence of previously formed particles and reduction of metal ions on the surface of the particles. It is supposed that metal reduction is much slower and the growth of NPs occurs preferably through silver reduction on their surface at lower

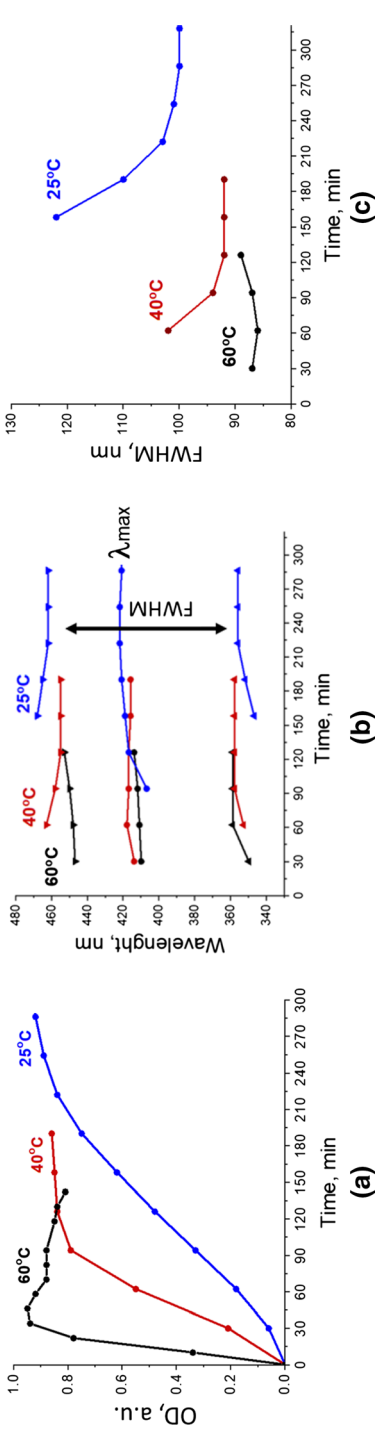

Fig. 2 The optical density growth of silver plasmon band (**a**), the changes of positions of band maximum and band borders at half-maximum (**b**) and the dependence of full width at half maximum (**c**) on irradiation time for Ag/Trp system obtained at 25 °C, 40 °C and 60 °C (278 nm, 1.0 mW/cm^2)

Table 1 The calculated time constants and the standard errors of fitted functions, exponential and sigmoid, that characterize growth profile of the process of silver nanoparticles formation in the Ag/Trp system under UV irradiation at 278 nm, output optical power density of 1.0 mW/cm^2 at different temperatures

	Exponential function (Adj-$R^2 = 0.9668$)	Sigmoid function (Adj-$R^2 = 0.9984$)
Temperature of reaction, °C	t, min	t, min
25	104.6 ± 15.0	113.0 ± 2.0
40	48.6 ± 13.9	46.7 ± 1.5
60	11.7 ± 3.3	11.5 ± 1.0

temperatures. In the case of Ag NPs obtained at 60 °C, the decrease of LSPR intensity can be connected with the decrease of the number of particles due to consumption of quickly formed small ones during coalescence.

When the photochemical process of particle formation is faster, LSPR maximum is more blue-shifted (Fig. 2b), namely the maxima of plasmon bands were located at 412 nm, 416 nm and 422 nm (Fig. 1b) at 60 °C, 40 °C and 25 °C, respectively. The LSPR band is not symmetrical in relation to the position of the band maximum. For instance, considering the full width of the band at its half maximum (FWHM), the distances from λ_{max} to band borders are not equal, the short wavelength section is almost twice bigger than the long wavelength section (Fig. 2b).

Also, when the process is slower, the LSPR band is broader, that is reflected in Fig. 2b and c as an increase of the value of FWHM with the temperature decrease. For instance, the smallest halfwidth of 86 nm was observed for Ag NPs obtained at 60 °C, while 92 nm and 100 nm were noted for the reaction at 40 °C and 25 °C, respectively.

According to the theory, the halfwidth of the plasmon band is inverse to the particle size, therefore its decrease in time for the same system is related to growth of silver nanoparticles (Fig. 2c). However, the comparison between real systems is much more complicated since the absorption of metal colloids includes the absorption of nanoparticles of different sizes (and/or shapes). Thus, the band halfwidth is connected not only with size, but also with the dispersity of colloids and nanoparticles heterogeneity. Analyzing optical characteristics of plasmon bands of obtained colloids, we can suggest that the formation of smaller and more uniform particles occurs when the reactive mixture is irradiated at the higher temperature (60 °C). In addition, the appearance of new absorption maxima at 329 nm should be noted with the decrease of the reaction temperature (25 °C and 40 °C) in the region of 300–350 nm (Fig. 1b).

As known from literature, changes in optical spectra are related to the morphology of NPs, moreover, the absorption band in the range of 300–350 nm have several interpretations for the systems containing nanosized silver. Authors of [9] observed LSPR shoulder peak at 345 nm for an aqueous suspension of 40 nm cubic seeds of silver (dipole resonance mode). In [10] the absorption at 340 nm was assigned to a transverse plasmon band of silver nanorods. Also, silver nanowires with similar

spectrum were described in [11]. Silver nanowires and silver-containing nanobars described in [12] and [13] also possessed such spectral features. Silver nanoprisms as well have a sharp plasmon band at 333 nm [14] assigned to one of the modes of out-of-plane quadrupole resonance.

Analyzing TEM images of prepared systems (Fig. 3), we concluded that the decrease in the reaction temperature from 60 to 25 °C caused nearly 2.5 times increase in average particle size from 20 to 50 nm and their inhomogeneity. We also observed "closely packed" nanoparticles obtained at 25 °C compared to clearly separated at 60 °C. Thus, the growth of absorption bands in the range of 300–350 nm is connected with the formation of elongated structures (chains, analogous of nanowires) composed from spherical nanoparticles.

Tryptophan in an aqueous solution adjusted to high pH exists in anionic form having a nonbonding pair of electrons on the nitrogen atom of the amino group and deprotonated carboxylic group –COO^-, that are involved in donor–acceptor bonds with *d*-orbitals of the metal. Reduction of metal ions proceeds through an indole ring. The formation of Ag NPs of non-uniform size is connected with competing processes of metal reduction and metal-Trp complexation, that affect the mechanism of particles nucleation and growth. At low temperatures, the reduction process proceeds slower, that promotes the growth of bigger particles due to reduction of silver ions on the surface of previously formed ones.

Tryptophan molecules can act as a bridge between surfaces of different NPs causing the aggregates' formation that was fixed on size distributions obtained by DLS, namely on an intensity basis (Fig. 4c). As a more effective reduction

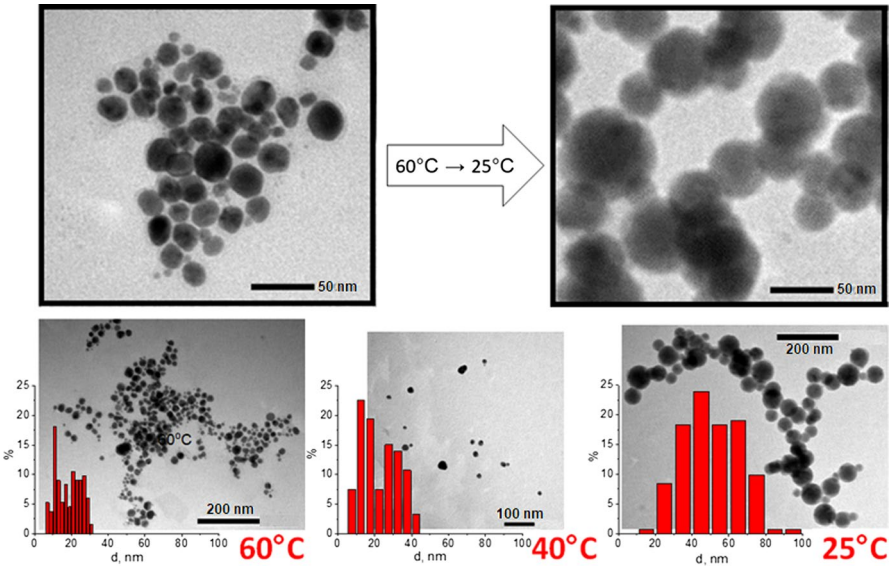

Fig. 3 TEM images of Ag NPs obtained under UV irradiation at 60, 40 and 25 °C and corresponding size distributions calculated by ImageJ (the number of analyzed particles for different temperatures—133, 93 and 142, respectively)

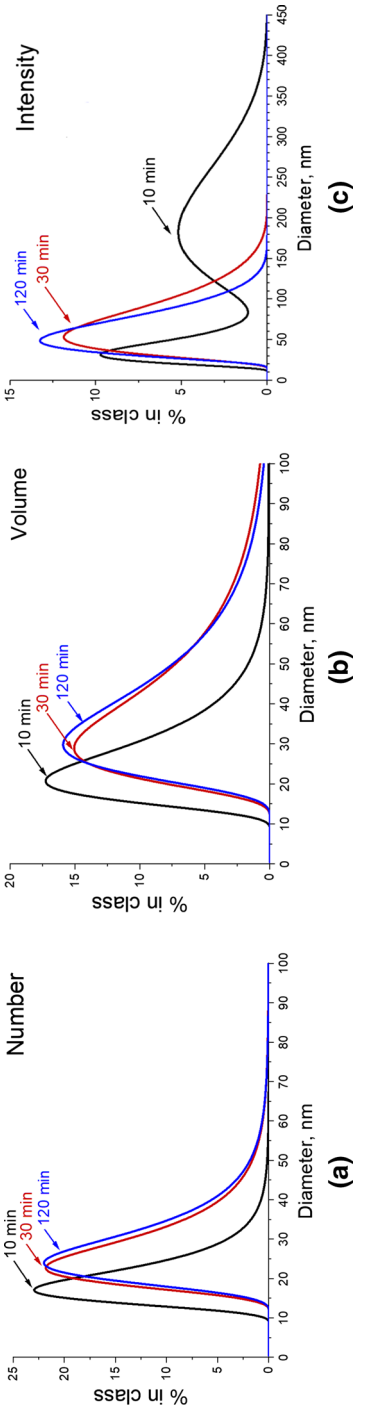

Fig. 4 The size distribution of Ag NPs by DLS method by number (**a**), volume (**b**) and intensity basis (**c**). Ag NPs were obtained photochemically at 60 °C during 10, 30 and 120 min of irradiation

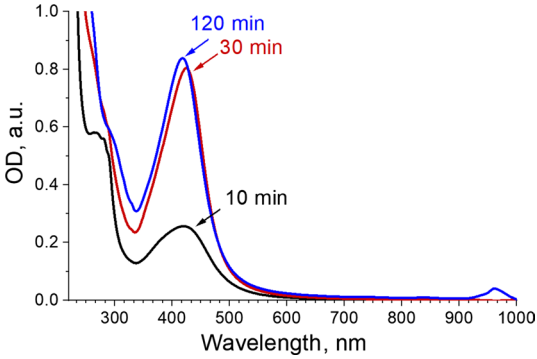

Fig. 5 The optical density spectra of Ag NPs colloids obtained in the presence of tryptophan at 60 °C under UV irradiation at 278 nm and 1.0 mW/cm^2 during 10 (**a**), 30 (**b**) and 120 min (**c**)

process requires more molecules to be activated with UV irradiation, it is important to apply irradiation with optimal duration. For instance, under applied experimental conditions, UV irradiation for 10 min is not enough to prepare colloids with monodisperse particles due to the abovementioned competing processes. There are two fractions on DLS plots of colloid irradiated for 10 min: small particles of 15–20 nm and aggregated particles of 100–350 nm (the most probable structure is chain-like) in comparison with the long term (30 min and 120 min) irradiated colloids where only one fraction of particles in the size of 25–30 nm is observed (Fig. 4c).

The size distribution plots are in agreement with absorption spectra, the spectrum of the aggregated sample contained low intense and broad LSPR bands compared to pronounced bands for more uniform dispersion (Fig. 5). This effect can be explained by the unfinished process of Ostwald ripening and the existence of unreduced metal ions [8]. We believe that this can be connected with the possible formation of aggregates or chain-like structures analogously to the process conducted at 25 °C.

Thus, according to optical density growth of LSPR and size distribution, the duration of UV irradiation should be at least 30 min to produce a more homogeneous colloid.

By varying the output optical power density of UV irradiation, the time profile of the reaction and the resulting optical properties as well as morphology of Ag NPs can be affected and tailored. The time-dependent spectra of the Ag/Trp system obtained at 60 °C with output optical power density of 0.4, 0.6 and 1.0 mW/cm^2 at 278 nm are presented in Fig. 6.

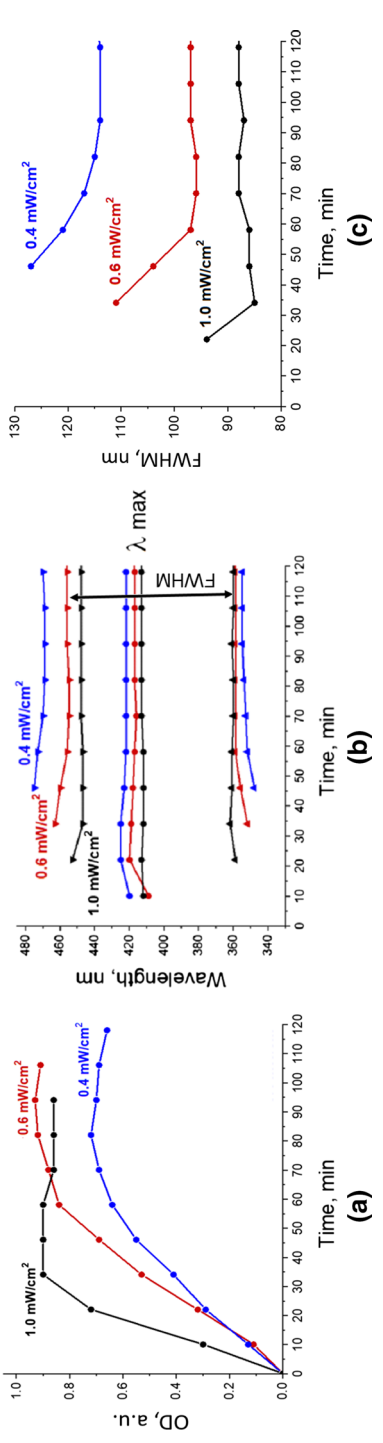

Fig. 6 The optical density growth of the silver plasmon band (**a**), the changes of positions of band maximum and band borders at half-maximum (**b**) and the dependence of full width at half maximum (**c**) on irradiation time for the Ag/Trp system obtained at 60 °C with output optical power density: 0.4, 0.6 and 1.0 mW/cm^2 at 278 nm

Table 2 The calculated time constants and the standard errors of fitted functions, exponential and sigmoid, that characterize the growth profile of the process of silver nanoparticles formation in Ag/Trp system at 60 °C under UV irradiation at 278 nm with different output optical power densities

	Exponential function (Adj-$R^2 = 0.9665$)	Sigmoid function (Adj-$R^2 = 0.9949$)
P, mW/cm^2	t, min	t, min
0.4	31.3 ± 6.0	26.2 ± 1.5
0.6	24.8 ± 4.1	21.0 ± 4.3
1.0	13.0 ± 3.8	12.3 ± 1.2

According to calculated time constants, formation of Ag NPs under UV irradiation at $\lambda = 278$ nm and 60 °C occurred app. 1.2 times faster with increase of the output optical power density from 0.4 to 0.6 mW/cm^2 and app. 1.7 times—from 0.6 to 1.0 mW/cm^2 (Table 2). The kinetics of optical density growth match the sigmoidal growth profile (Adj-$R^2 = 0.9949$) which is in better agreement with experimental values comparde to exponential fit (Adj-$R^2 = 0.9665$). The Adj-R^2 is an estimate of goodness of fit and this value is suitable for comparing the different fitting models.

The decrease of UV irradiation intensity, namely the output optical power density of UV-C LED, affected the systems similar to the decrease of temperature. The UV illumination with lower power caused slower LSPR band growth, broader band width and red-shifted the LSPR maximum (Fig. 6).

Such a process was reflected in DLS distribution (Fig. 7) as the growth of Ag NPs size and inhomogeneity with the decreasing of optical power density.

The conducted investigation showed that properties of silver colloids obtained in the photochemical process between Ag^+ and Trp can be affected by thermodynamic (temperature) and kinetic (reaction rate according to applied irradiation) parameters that define size/shape distribution of particles and, in turn, their optical features. Thus, UV light from a LED source is a promising tool for size/shape-controlled colloidal synthesis of noble NPs.

Conclusions

Photochemical activation of an Ag/Trp system at 278 nm corresponding to the absorbance maximum of indole moiety of Trp, allows obtaining the stable biocompatible silver nanoparticles in an aqueous medium at relatively low temperatures. Whereas, the plasmon absorption band of Ag NPs was not observed at 25 °C during chemical reaction, the photochemical activation provides its steady growth. Under UV irradiation, the process of Ag NPs formation can be accelerated up to 10 times with an increase of the temperature from 25 to 60 °C. When the process occurs faster, LSPR maximum is more blue-shifted: 412 nm, 416 nm and 422 nm under 60, 40 and 25 °C, respectively. It is found that the formation of smaller and more uniform particles with diameters about 25–30 nm occur when

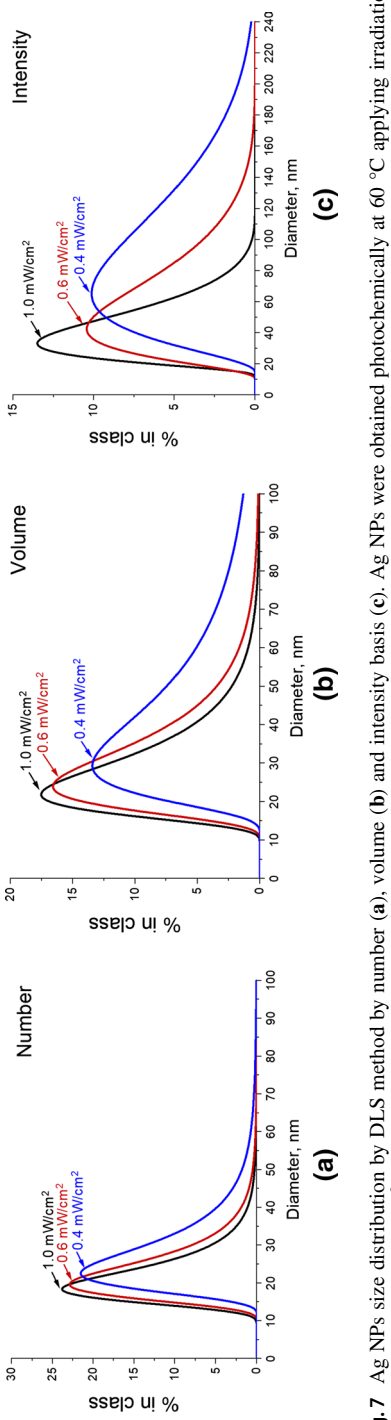

Fig. 7 Ag NPs size distribution by DLS method by number (**a**), volume (**b**) and intensity basis (**c**). Ag NPs were obtained photochemically at 60 °C applying irradiation with 0.4, 0.6 and 1.0 mW/cm^2

the reactive mixture is irradiated at higher temperature (60 °C) at 278 nm and 1.0 mW/cm^2 for more than 30 min. The optimal UV irradiation parameters and temperature of reaction can be chosen for the synthesis of colloids with tailored dispersity and optical properties.

Acknowledgements The authors are grateful to S. Kolotilov and R. Barakov for the support of the DLS study. National Academy of Sciences of Ukraine supported this work in the framework of grants of NASU for the research laboratory/group of young scientists of NASU for conducting investigations in priority directions of science and technology development in 2018–2019 (No. 29/2018-2019).

References

1. K. Sztandera, M. Gorzkiewicz, B. Klajnert-Maculewicz, Mol. Pharm. **16**, 1 (2018)
2. G. Vlăsceanu, S. Marin, R. Ţiplea, I. Bucur, M. Lemnaru, M. Marin, E. Andronescu, Silver nanoparticles in cancer therapy, in *Nanobiomaterials in Cancer Therapy. Application of Nanobiomaterials*, ed. by A. Grumezescu (Elsevier, Amsterdam, 2016), p. 588
3. I. Shmarakov, I. Mukha, N. Vityuk, V. Borschovetska, N. Zhyshchynska, G. Grodzyuk, A. Eremenko, Nanoscale Res. Lett. **12**, 333 (2017)
4. I. Mukha, N. Vityuk, G. Grodzyuk, S. Shcherbakov, A. Lyberopoulou, E.P. Efstathopoulos, M. Gazouli, J. Nanosci. Nanotechnol. **17**, 8987 (2017)
5. A. Lyberopoulou, S. Grammaticaki, I. Mukha, N. Vityuk, L. Pylypchuk, L. Storozhuk, V. Kouloulias, M. Gazouli, Pharmakeftiki **29**(4), 61 (2017)
6. H. Katifelis, A. Lyberopoulou, I. Mukha, N. Vityuk, G. Grodzyuk, G.E. Theodoropoulos, E.P. Efstathopoulos, M. Gazouli, Artif. Cell Nanomed. **46**, 389 (2018)
7. I. Mukha, N. Vityuk, O. Severynovska, A. Eremenko, N. Smirnova, Nanoscale Res. Lett. **11**, 101 (2016)
8. N.T.K. Thanh, N. Maclean, S. Mahiddine, Chem. Rev. **114**, 7610 (2014)
9. X. Xia, J. Zeng, Q. Zhang, C.H. Moran, Y. Xia, J. Phys. Chem. **116**, 21647 (2012)
10. Z. Jiang, G. Wen, Y. Luo, X. Zhang, Q. Liu, A. Liang, Sci. Rep. **4**, 5323 (2014)
11. B.J. Wiley, S.H. Im, Z. Li, J. McLellan, A. Siekkinen, Y. Xia, J. Phys. Chem. **110**, 15666 (2006)
12. J.P. Deng, S.H. Li, S.T. Chang, Y.C. Shih, Res. Chem. Intermed. **45**, 119 (2019)
13. J.P. Deng, J.-H. Lin, C.-Y. Hsu, Res. Chem. Intermed. **40**, 2269 (2014)
14. N.B. Bakar, J.G. Shapter, M.M. Salleh, A.A. Umar, Appl. Sci. **5**, 209 (2015)

Affiliations

Iu. Mukha[1] · N. Vityuk[1] · A. Khodko[2] · O. N. Kachalova[2,4] · O. Fedyshyn[3] · M. Malysheva[3] · A. Eremenko[1]

A. Khodko
khodkoalina@gmail.com

O. N. Kachalova
kachalova.nataliya@gmail.com

M. Malysheva
maria_malysheva@univ.kiev.ua

[1] Chuiko Institute of Surface Chemistry, NAS of Ukraine, 17 General Naumov Str., Kiev 03164, Ukraine

[2] Institute of Physics, NAS of Ukraine, pr. Nauky, 46, Kiev 03039, Ukraine

[3] Department of Chemistry, Taras Shevchenko National University of Kyiv, 64 Volodymyrska Str., Kiev 01601, Ukraine

[4] L.M. Litvinenko Institute of Physical - Organic and Coal Chemistry, NAS of Ukraine, 40 Kharkivske Shose Av, Kiev 02160, Ukraine